CHAPTER EIGHTEEN

Genetically Encoded Spin Labels for *In Vitro* and In-Cell EPR Studies of Native Proteins

M.J. Schmidt, A. Fedoseev, D. Summerer, M. Drescher[1]
Department of Chemistry, Zukunftskolleg, and Konstanz Research School Chemical Biology, University of Konstanz, Konstanz, Germany
[1]Corresponding author: e-mail address: malte.drescher@uni-konstanz.de

Contents

Abstract

Electron paramagnetic resonance (EPR) spectroscopy in combination with site-directed spin labeling (SDSL) is a powerful approach to study the structure, dynamics, and interactions of proteins. The genetic encoding of the noncanonical amino acid spin-labeled lysine 1 (SLK-1) eliminates the need for any chemical labeling steps in SDSL–EPR studies and enables the investigation of native, endogenous proteins with minimal structural perturbation, and without the need to create unique reactive sites for chemical labeling. We report detailed experimental procedures for the efficient synthesis of SLK-1, the expression and purification of SLK-1-containing proteins under conditions that ensure maximal integrity of the nitroxide radical moiety, and procedures for intramolecular EPR distance measurements in proteins by double electron–electron resonance.

1. INTRODUCTION

Electron paramagnetic resonance (EPR) distance measurements of spin-labeled proteins provide valuable insights about the structure, dynamics, and interactions of proteins and protein complexes in the noncrystalline

Methods in Enzymology, Volume 563
ISSN 0076-6879
http://dx.doi.org/10.1016/bs.mie.2015.05.023

state (Hubbell, Cafiso, & Altenbach, 2000; Jeschke, 2012). However, a prerequisite for the studying of proteins by EPR spectroscopy is the presence of paramagnetic centers. Site-directed spin labeling (SDSL) EPR enables studying the structure and dynamics of proteins which do not contain native paramagnetic centers. Distance measurements between two spin labels rely on their dipole–dipole coupling that is inversely proportional to the cube of their distance. Pulsed EPR techniques can be used to separate the dipole–dipole interaction from other contributions of the spin Hamiltonian and thereby provide information on distances in the 1.5–10 nm range. The most widely used approach for EPR distance measurements is double electron–electron resonance (DEER, synonymously used with pulsed electron double resonance [PELDOR]) (Jeschke, 2002; Jeschke, Abbott, Lea, Timmel, & Banham, 2006; Jeschke, Bender, Paulsen, Zimmermann, & Godt, 2004).

A variety of approaches of SDSL have previously been developed and established. Traditionally, unique cysteines in proteins are reacted with thiole-reactive reagents such as the methanethiosulfonate spin label (MTSSL) *in vitro* (Altenbach, Marti, Khorana, & Hubbell, 1990). However, this requires the deletion of native cysteins and the introduction of new cysteins at the desired sites by mutagenesis. Since cysteines carry out various essential functions in proteins, such as serving as redox-active or nucleophilic catalytic centers, as stabilizers of protein folds or as metal ion ligands, this prevents the investigation of various proteins in their natural state (Pace & Weerapana, 2013). Spin labels can also be introduced as amino acids by chemical protein (semi)-synthesis (Klare & Steinhoff, 2009), nonsense codon suppression with chemically aminoacylated tRNAs (Cornish et al., 1994; Shafer, Kalai, Liu, Hideg, & Voss, 2004) or by conjugation to genetically encoded, noncanonical amino acids (ncAA) containing aldehydes and azides (Fleissner et al., 2009; Kalai, Fleissner, Jeko, Hubbell, & Hideg, 2011). Finally, nitroxides have been introduced into proteins by complexation with His tags (Baldauf, Schulze, Lueders, Bordignon, & Tampe, 2013). However, these approaches employ mandatory chemical labeling steps *in vitro* and thus do not fully meet the aspiring goals of protein SDSL–EPR studies, that is, studying proteins in their native folding state, with minimal structural modification, and directly in the unperturbed, intracellular environment of their host cells.

We recently reported the direct biosynthesis of spin-labeled proteins in live *Escherichia coli* cells, overcoming the aforementioned limitations of *in vitro* spin labeling (Schmidt, Borbas, Drescher, & Summerer, 2014). This technique relies on the genetic encoding of the spin-labeled amino acid

SLK-1 (Fig. 1A) in response to the amber stop codon (TAG) (Liu & Schultz, 2010) by an evolved, orthogonal $tRNA^{Pyl}$/pyrrolysyl-tRNA-synthetase (PylRS) pair (Blight et al., 2004; Chen et al., 2009; Fekner, Li, Lee, & Chan, 2009; Gautier et al., 2010; Hoppmann et al., 2014; Li et al., 2013; Luo et al., 2014; Plass et al., 2012; Polycarpo et al., 2006; Pott, Schmidt, & Summerer, 2014; Schmidt & Summerer, 2013; Wan et al., 2010; Wan, Tharp, & Liu, 2014; Yanagisawa et al., 2008). This enables the cotranslational incorporation of SLK-1 at single and multiple user-defined sites of proteins with high efficiency and fidelity. Possible applications of SLK-1 can best be described by a brief survey of our recent experiments.

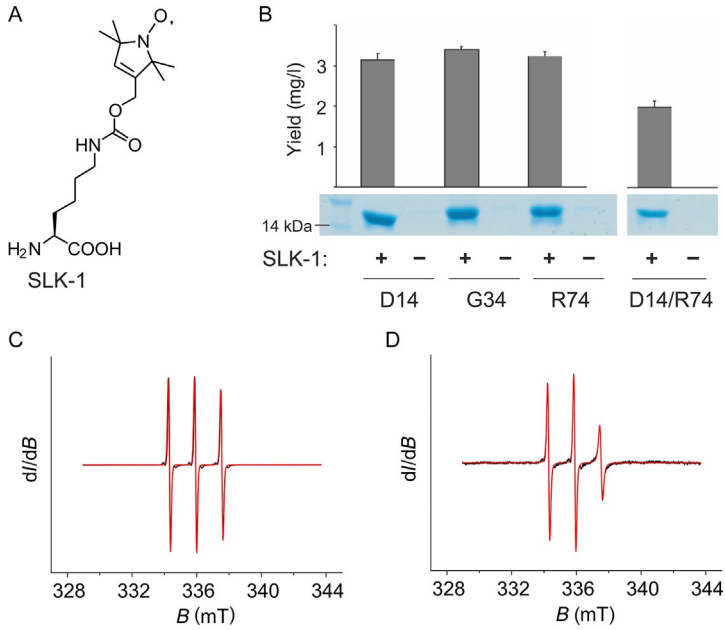

Figure 1 Cotranslational incorporation of spin-labeled amino acid SLK-1 into proteins in *E. coli*. (A) Chemical structure of SLK-1. (B) Incorporation of SLK-1 in *E. coli* thioredoxin at user-defined sites. TRX mutants with amber codons at indicated positions and with C-terminal His6 tag were coexpressed with $tRNA^{Pyl}$/PylRS-SL1 in *E. coli* in the presence of SLK-1. Yields of protein expressions in the presence of SLK-1 obtained from BCA assays are shown as gray bars. SDS-PAGE analysis of proteins purified by Ni-NTA chromatography is shown at the bottom of the figure. (C) EPR spectrum of SLK-1 in buffer. (D) EPR spectrum of purified TRX-D14 → SLK-1 in buffer. X-band spectra at room temperature and spectral simulations for panels (C and D) are shown in black and red (gray in the print version), respectively.

We investigated the incorporation of SLK-1 into *E. coli* thioredoxin (TRX) and performed structural studies by DEER, since this enzyme serves as important oxidoreductase in various redox processes including dithiole–disulfide exchange reactions. Furthermore, X-ray structural information for this protein is available for data comparison (Katti, LeMaster, & Eklund, 1990), and the catalytic center of TRX is constituted by two redox-active cysteines. This prohibits structural studies of the native protein by traditional MTSSL labeling and DEER (Katti et al., 1990). Finally, TRX is a homologous protein in *E. coli*, which could be studied with minimal perturbation of its natural environment and in its natural host cells, where it is biosynthesized and processed.

By coexpression of $tRNA^{Pyl}$/PylRS-SL1 in the presence of SLK-1 with genes encoding TRX bearing a C-terminal His6 tag and containing amber codons at different positions, spin-labeled TRX proteins are obtained with good yields and purities after Ni-NTA purification, as indicated by SDS-PAGE analysis and a bicinchoninic acid (BCA) assay (Fig. 1B). Yields of SLK-1-containing TRX mutants are in the range of 2–3 mg/l expression culture for singly labeled proteins; doubly labeled TRX proteins are typically obtained with yields of >1 mg/l. Studies with other target proteins typically afforded yields of >1 mg/l, being in a reasonable range for EPR studies (e.g., green fluorescent protein and T4 lysozyme, data not shown). Typically, expression yields of SLK-1-containing proteins are reduced compared to the expression of the wild-type proteins due to competition of $tRNA^{Pyl}$ with release factor 1 (RF1) (Liu & Schultz, 2010). A number of strategies have been developed to increase the efficiency of amber suppression with ncAA that may be employed, if higher yields are required. Besides optimizing expression levels of tRNA and aminoacyl-tRNA-synthetase (aaRS) (Cellitti et al., 2008; Chatterjee, Sun, Furman, Xiao, & Schultz, 2013; Ryu & Schultz, 2006; Young, Ahmad, Yin, & Schultz, 2010), these include the optimization of tRNAs (Chatterjee et al., 2013; Guo, Melancon, Lee, Groff, & Schultz, 2009), reduced amber codon recognition by RF1 by its genomic knockout (Johnson et al., 2012, 2011; Lajoie et al., 2013; Mukai et al., 2010), by engineering RF1 itself (Ryden & Isaksson, 1984; Wu et al., 2013; Zhang, Ryden-Aulin, Kirsebom, & Isaksson, 1994), or its binding site at the ribosome (Huang et al., 2010; Wang, Neumann, Peak-Chew, & Chin, 2007), and optimization of the sequence context of the amber codon (Pott et al., 2014).

In EPR measurements, the spectral shape of free SLK-1 corresponds to a fast tumbling small molecule, as expected (Fig. 1C). Spectral simulations (Stoll & Schweiger, 2006) revealed a rotational correlation time $\tau_c = 40$ ps. The EPR spectrum for SLK-1 incorporated into *E. coli* TRX shows a comparably low mobility of the nitroxide moiety (Fig. 1D, $\tau_c = 250$ ps). For structural investigations of *E. coli* TRX by DEER, purified, doubly labeled protein (e.g., TRX-D14/R74→SLK-1) is dialyzed into aqueous buffer. Before shock freezing in liquid nitrogen in order to trap the macromolecular conformation, 20% (v/v) glycerol was added to obtain a glassy matrix. The DEER measurements were performed at $T = 50$ K to optimize relaxation rates of the spin system and to avoid reorienting of the spin–spin interconnecting vector due to molecular tumbling. The latter would average the dipole–dipole interaction which is required for distance determination. Depending on the labeling strategy adopted, both intermolecular and intramolecular distances can be measured. Distances between molecules can, in fact, be obtained from proteins with a single SLK-1 incorporated. Double incorporation of SLK-1 can instead be used to measure distances within proteins. When measuring intramolecular distances, the contribution of distances to neighboring proteins should be suppressed. Therefore, a singly labeled control protein (e.g., TRX-D14→SLK-1) is required for control measurement. For TRX-D14→SLK-1, obtained DEER data are in full agreement with a homogeneous 3D distribution of spin labels as expected for a singly labeled protein in solution. For TRX-D14/R74→SLK-1 (Fig. 2A), the background corrected DEER data result in the corresponding distance distributions by model-free analyses using DEERAnalysis2013 (Fig. 2B; Jeschke et al., 2006).

An important aspect of SDSL–EPR is the influence of the linker flexibility of a spin label on the distance distribution. This factor can be predicted via rotamer approaches (Polyhach, Bordignon, & Jeschke, 2011).

In case of SLK-1, the experimental distance distribution for TRX-D14/R74→SLK-1 is in agreement with the theoretically predicted distance distribution between traditional MTSSL moieties at the same incorporation sites (Fig. 2B). More importantly, a direct experimental comparison between TRX-D14/R74→SLK-1 and the corresponding MTSSL-labeled mutant TRX-C33S/C36S/D14C/R74C exhibits a similar distance distribution (Fig. 2C). For the latter protein, additional maxima are observed that were identified as artifacts caused by oligomerization via disulphide bridges

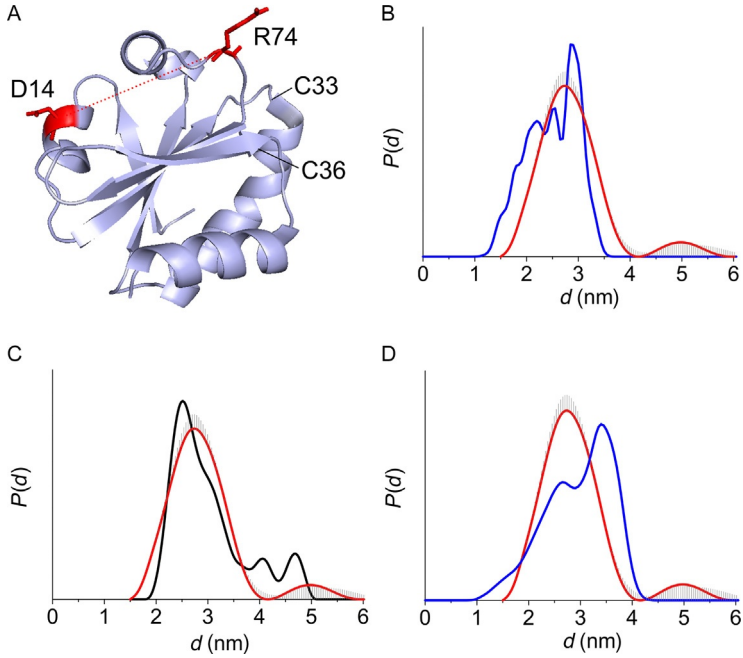

Figure 2 DEER distance measurements in *E. coli* thioredoxin (TRX). (A) Cartoon representation of the crystal structure of TRX (pdb entry 2TRX) (Katti et al., 1990). Amino acids at both incorporation sites of SLK-1 (D14 and R74) are shown as sticks, the corresponding Cα–Cα distance is indicated as dotted red line. Positions of catalytic cysteines C33 and C36 are indicated. (B) Distance distribution for TRX-D14/R74→SLK-1 (red) compared to the theoretically predicted distance distribution between two MTSSL moieties at corresponding positions (blue). (C) Distance distribution for TRX-D14/R74→SLK-1 (red) compared to the distance distribution of MTSSL-labeled TRX-C33S/C36S/D14C/R74C (black). (D) Distance distribution for TRX-D14/R74→SLK-1 (red) compared to the theoretically predicted distance distribution between two SLK-1 at the same positions (blue).

during the labeling protocol. This effect was not observed for TRX-D14/R74→SLK-1, where an introduction of surface-exposed cysteines is not required. These data indicate that SLK-1 is a useful structural probe with similar spectral characteristics as MTSSL and that SLK-1-based DEER measurements can deliver insights without artifacts from chemical labeling steps associated with MTSSL. To further analyze the flexibility of the SLK-1 side chain (Polyhach et al., 2011), we established rotamer libraries for the prediction of SLK-1 distance distributions on the basis of a model of the protein structure (Fig. 2D).

Recent studies have shown that singly SLK-1-labeled proteins can selectively be detected in the host *E. coli* cells where they are biosynthesized and

processed (Schmidt et al., 2014). Thorough washing of cells with Luria Broth (LB) media reduced background signals arising from free SLK-1 in *E. coli*, as indicated by measurements of control expressions that did not include SLK-1, an amber codon in the target TRX gene, or the plasmid for coexpression of the $tRNA^{Pyl}$/PylRS-SL1 pair (Fig. 3A). These experiments indicate that our approach affords sufficient expression levels of endogenous, spin-labeled proteins for *in-cell* SDSL–EPR measurements and that free SLK-1 can be selectively washed out of cells under conditions that leave the spin-labeled protein intact and localized in the cells. This provides a starting point for future *in-cell* EPR studies of proteins with increased

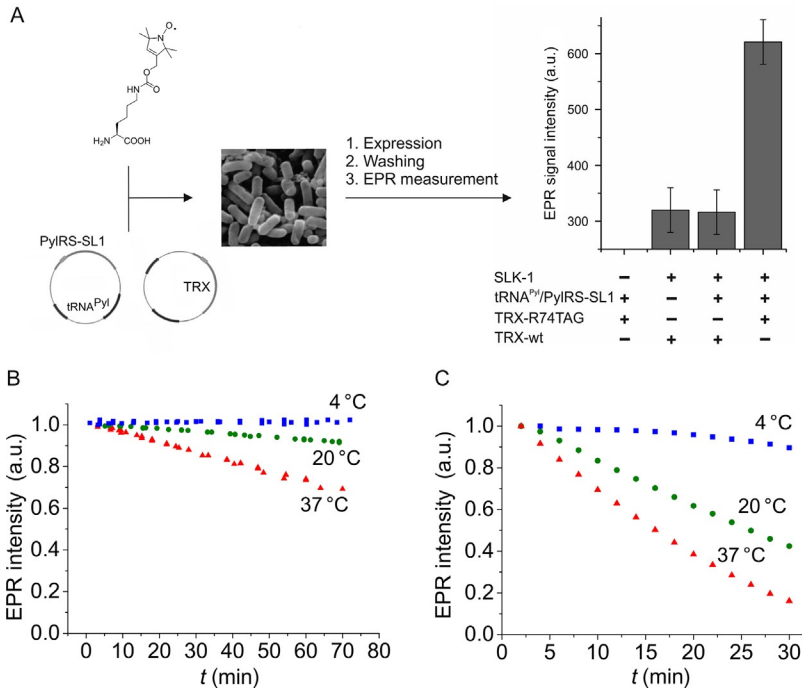

Figure 3 Detection of SLK-1-labeled proteins in *E. coli* and stability of SLK-1 under conditions of protein expression in *E. coli*. (A) Cartoon: workflow of the sample preparation for EPR measurements of intracellular TRX-R74 → SLK-1. Plasmids encoding $tRNA^{Pyl}$, PylRS-SL1, and TRX-R74 → TAG are transformed into *E. coli*, and proteins are expressed in the presence of SLK-1. Cells are washed with LB media, pelleted, and subjected to EPR measurements. Diagram: EPR signal intensities for EPR measurements of washed *E. coli* cells with negative controls omitting SLK-1, the amber codon at position 74 or the $tRNA^{Pyl}$/PylRS-SL1 pair as shown in the figure. a.u. = arbitrary units. (B) EPR signal decay for free SLK-1 in *E. coli* culture in LB medium at temperatures as indicated. (C) EPR signal decay for free SLK-1 in pelleted and lysed (uncleared) *E. coli* lysates at temperatures as indicated.

biorelevance, i.e., without the need for microinjection of *in vitro* spin-labeled molecules into *Xenopus* oocytes or transfection protocols (Azarkh et al., 2011, 2012, 2013; Igarashi et al., 2010; Krstic et al., 2011; Martorana et al., 2014; Qi, Groß, Jeschke, Godt, & Drescher, 2014).

A critical property of nitroxides for EPR studies in biological environments is the stability of the radical moiety. Nitroxides have been reported to be prone to chemical conversion in all previously studied intracellular contexts (Belkin, Mehlhorn, Hideg, Hankovsky, & Packer, 1987; Couet, Brasch, Sosnovsky, & Tozer, 1985; Krstic et al., 2011), resulting in signal decay (loss of paramagnetism). This limits the sensitivity and applicable maximal measurement times of SDSL–EPR studies of proteins. SLK-1-containing proteins expressed in *E. coli* typically exhibit integrity degrees of ~50–70% (the integrity degree is defined as the percentage of intact, paramagnetic SLK-1 per initially incorporated SLK-1). Note that the *labeling* degree with SLK-1, i.e., the incorporation without taking into account potential conversion of the radical, is determined by the translation fidelity and thus is >99%) (Schmidt et al., 2014). However, the overall integrity degree for doubly labeled proteins is decreasing in a multiplicative manner compared to singly labeled proteins and this can prevent successful DEER measurements. It is thus very important to take any measures that prevent SLK-1 conversion during protein expression, lysis, and purification. Signal decay measurements with free SLK-1 in *E. coli* expression cultures or in lysed, uncleared *E. coli* cells indicate that both temperature and incubation time are critical parameters that affect the integrity degree (Fig. 3B and C). For high degrees, minimal expression temperature and times are recommended, as well as a fast lysis and purification protocol at low temperature. Additionally, the presence of serine protease inhibitors such as phenylmethylsulfonyl fluoride (PMSF) or 4-(2-aminoethyl)benzensulfonylfluoride (AEBSF) during lysis has been observed to strongly decrease the undesired conversion of free SLK-1 (data not shown).

2. EXPERIMENTAL GUIDELINES

Here, we provide detailed experimental guidelines on how the genetically encoded spin label SLK-1 can be used to obtain long-range distance constraints for structural studies of native, endogenous proteins. The entire experimental design starting from the synthesis of SLK-1 via genetic encoding, protein expression, and EPR measurements to data analysis is described.

2.1 Precautions

For reliable results and maximal yields in the organic synthesis of SLK-1, all described organic reactions should be performed under anhydrous conditions and an inert atmosphere of argon in oven-dried glassware with magnetic stirring. During the expression and purification of SLK-1-containing proteins, the exposure of SLK-1 to air and cell media should be kept to a minimum to obtain maximal integrity degrees. SLK-1 should be added only shortly before induction of protein expression, and expression time should be minimal and at the minimal possible temperature. Most importantly, the lysis and purification have to be performed as fast as possible, at 4 °C, and PMSF should be included during lysis. Once purified, SLK-1 is stable in proteins at room temperature, but storage temperature should be as low as possible as a precaution. Note that the use of any reductants such as dithiothreitol (DTT) or β-mercaptoethanol will reduce SLK-1 to the EPR-inactive hydroxylamine. As for all labeling techniques, control experiments aimed at excluding distortions of the original protein behavior due to incorporation of SLK-1 are essential.

2.1.1 Experimental Strategy

Most promising labeling positions are those that result in distance distributions that fall in the optimum distance range (1.5–6 nm). For their identification, analyzing high-resolution structural models, for instance, those obtained from the pdb database (http://www.rcsb.org/pdb/) may be a good starting point.

2.2 Organic Synthesis

Nitroxide amino acid SLK-1 can be synthesized from commercially available starting materials by *N*,*N*′-disuccinimidyl carbonate-(DSC)-mediated carbamate formation between 3-hydroxymethyl-1-oxy-2,2,5,5-tetramethylpyrroline and Nα-Boc-protected L-lysine, followed by deprotection with trifluoroacetic acid (Fig. 4).

This protocol affords SLK-1 with high purity and with an overall yield of 84%. The reaction outcome of the carbamate coupling step can be quickly assessed by TLC and high-resolution mass spectrometry (HRMS). The final product can additionally be analyzed by ^{1}H and ^{13}C NMR after a reduction to the hydroxylamine with formic acid to confirm the identity and ensure high purity of SLK-1 for subsequent molecular biology experiments.

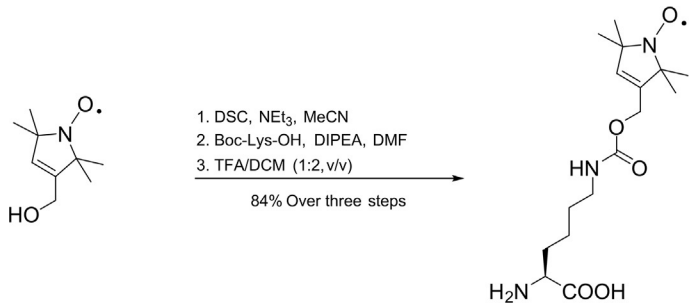

Figure 4 Scheme of synthesis of nitroxide amino acid SLK-1 from commercially available starting materials.

2.2.1 Materials

Reagents were purchased from the following suppliers: 2,2,5,5-tetramethyl-3-pyrrolin-1-oxyl-3-carboxylic acid was purchased from Acros Organics; Red-Al® sodium bis(2-methoxyethoxy)aluminum hydride solution (≥60 wt.% in toluene) and trifluoroacetic acid were purchased from Sigma-Aldrich; *N*,*N*′-disuccinimidyl carbonate, 98%, and *N*,*N*-diisopropylethylamine, 99%, were purchased from Abcr; and triethylamine was purchased from Merck. Flash chromatography: Roth 60 F254 (230–400 mesh) silica gel. Solvents used for chromatography were ethyl acetate, DCM, and methanol, technical grade. Reaction solvents were purchased in anhydrous quality and stored over molecular sieve. Acetonitrile, toluene, and DMF were purchased from Sigma-Aldrich. ^{1}H and ^{13}C NMR spectra were recorded at ambient temperature on a Bruker Avance III 400 instrument. Signal positions are reported in δ/ppm with their characteristics denoted as s (singlet), d (doublet), dd (double doublet), t (triplet), m (multiplet), and br (broad). HRMS measurements were performed on a Bruker Daltonics micrOTOF II. DCM, dichloromethane; TLC, thin-layer chromatography; MeOH, methanol; and TFA, trifluoroacetic acid.

2.2.2 Synthesis of Nitroxide Amino Acid SLK-1

(a) Carbamate coupling step

1. Dissolve 3-hydroxymethyl-1-oxy-2,2,5,5-tetramethyl-pyrroline (3.6 g, 21.14 mmol, 1 equiv.) in acetonitrile (40 ml).
2. Add triethylamine (11.73 ml, 84.6 mmol, 4 equiv.) and cool the solution in an ice bath under argon atmosphere.
3. Add *N*,*N*′-disuccinimidyl carbonate (8.13 g, 31.72 mmol, 1.5 equiv.) in one portion and stir the solution at 0 °C, then at room temperature overnight (13 h).

4. Concentrate the reaction mixture under reduced pressure, dry *in vacuo*, and filter the residue through a pad of silica gel using ethyl acetate as solvent.
5. Concentrate the filtrate under reduced pressure, dissolve it in anhydrous DMF (20 ml), and add it dropwise to a suspension of Boc-Lys-OH (7.81 g, 31.72 mmol, 1.5 equiv.) and *N*,*N*-diisopropylethylamine (10.8 ml, 63.44 mmol, 3 equiv.) in anhydrous DMF (40 ml) at 0 °C.
6. Stir the reaction mixture for 20 h at room temperature.
7. Quench the reaction with water (300 ml) and extract it with ethyl acetate (6 × 100 ml). Wash the organic phase with water (4 × 200 ml) and dry over $MgSO_4$. Evaporate the solvent and purify the obtained yellow oil by flash column chromatography (DCM, DCM/1% MeOH → DCM/2% MeOH) to yield (*S*)-2-((*tert*-butoxycarbonyl)amino)-6-((((1-oxy-2,2,5,5-tetramethylpyrroline-3-yl)methoxy)carbonyl) amino)hexanoic acid as a yellow foam (7.94 g, 17.94 mmol, 85%). TLC (DCM/MeOH 95:5) Rf = 0.28. HR-ESI MS (*m*/*z*): $[M+H]^+$ calculated for $[C_{21}H_{37}N_3O_7]^+$: 443.2626, found: 443.2607. $[M+Na]^+$ calculated for $[C_{21}H_{36}N_3O_7 \cdot Na]^+$: 465.2446, found: 465.2432.

(b) Deprotection step

1. Dissolve (*S*)-2-((*tert*-butoxycarbonyl)amino)-6-((((1-oxy-2,2,5,5-tetramethylpyrroline-3-yl)methoxy) carbonyl)-amino)hexanoic acid (3.2 g, 7.23 mmol) in DCM (20 ml).
2. Add trifluoroacetic acid (6 ml) dropwise at room temperature and stir the reaction mixture for 40 min. Avoid longer reaction times and monitor the reaction progress by TLC to exclude undesired cleavage of the *N*ε-carbamate bond.
3. Remove the solvent and coevaporate the residual oil once with methanol (100 ml).
4. Add diethyl ether (5 × 100 ml) to the residual oil, decant the solvent, and dry the remaining oil in *vacuo* to obtain a white powder under reduced pressure. This yields the TFA salt of SLK-1 ((*S*)-2-amino-6-((((1-oxy-2,2,5,5-tetramethylpyrroline-3-yl)methoxy) carbonyl)amino)hexanoic acid) as a white foam (3.27 g, 7.16 mmol, 99%).HR-ESI MS (*m*/*z*): $[M+H]^+$ calculated for $[C_{16}H_{29}N_3O_5]^+$: 343.2102, found: 343.2091.

(c) Reduction of SLK-1 to corresponding hydroxylamine for NMR characterization

1. Dissolve SLK-1 (100 mg, 0.22 mmol) in 6 ml H_2O/formic acid (1:1, v/v) and stir for 24 h at room temperature.
2. Remove the solvent under reduced pressure and coevaporated 3 × with 50 m*M* HCl (15 ml) to afford the HCl salt of (*S*)-2-amino-6-((((1-hydroxy-2,2,5,5-tetramethylpyrroline-3-yl)methoxy) carbonyl)amino)hexanoic acid (81 mg, quant.). ^{1}H NMR (400 MHz, D_2O), δ: 5.90 (s, 1H, H–C═C–), 4.66 (m, 2H, $-CH_2-$), 3.71 (t, $J = 6.1$ Hz, 1H, Hα), 3.12 (t, $J = 6.7$ Hz, 2H, $-CH_2-$), 1.84 (m, 2H, $-CH_2-$), 1.63–1.25 (m, 16H, 2 × $-CH_2-$, 4 × $-CH_3$). ^{13}C NMR (101 MHz, D_2O), δ: 171.99, 157.67, 138.40, 129.27, 77.78, 76.05, 59.89, 52.73, 39.94, 29.34, 28.35, 23.98, 22.79, 21.60, 21.43, 21.39.

2.3 Expression and Purification of Spin-Labeled Proteins in *E. coli*

2.3.1 Materials

2.3.1.1 *E. coli* Strains and Expression Plasmids

E. coli strains GH371 and Top10 afford the described expression yields and integrity degrees of SLK-1-containing proteins. Other *E. coli* expression strains compatible with the used expression plasmids may be used, but yields and integrity degrees may differ, the latter owing to the unknown origin of nitroxide conversion in *E. coli*.

Expression of SLK-1-containing proteins requires the coexpression of $tRNA^{Pyl}$ and PylRS-SL1, a PylRS mutant previously evolved for the genetic encoding of SLK-1. Plasmid pEVOL_PylRS-SL1 (Schmidt et al., 2014) provides high-expression levels for this purpose, though other plasmids may be used. pEVOL-PylRS-SL1 (p15A origin of replication, chloramphenicol resistance) encodes $tRNA^{Pyl}$ under control of the proK promoter and two copies of PylRS-SL1 under control of a glnS′ promoter and an araBAD promoter, respectively (Young et al., 2010). In principle, the target protein can be expressed under control of various promoters from plasmids with compatible origin of replication. The described experiments made use of pBAD plasmids with ampicillin resistance and colE1 origin of replication (pBAD-TRX_D14/R74TAG, pBAD-TRX_D14TAG, or pBAD-TRX_R74TAG).

2.3.1.2 Culture Media, Reagents, and Lysis/Purification Buffers

Media and reagents were purchased from the following suppliers: LB media, carbenicillin, chloramphenicol, PMSF (phenylmethanesulfonylfluoride),

and Coomassie Brilliant Blue were purchased from Carl Roth; L-arabinose was purchased from Sigma-Alrich; B-Per lysis reagent was purchased from Thermo Scientific; imidazole was purchased from Abcr; Ni-NTA agarose slurry was purchased from Qiagen; and paper filter spin column and BCA assay were purchased from Pierce. Amicon Ultra centrifugal columns with a molecular weight cutoff of 3 kDa were purchased from Millipore.

(a) 4× PBS: 548 m*M* NaCl, 10.8 m*M* KCl, 40 m*M* Na_2HPO_4, 7.2 m*M* KH_2PO_4, pH 7.4.

(b) Wash buffer: 50 m*M* NaH_2PO_4, 300 m*M* NaCl, pH 8.0, containing 20 m*M* imidazole.

(c) Elution buffer: 50 m*M* NaH_2PO_4, 300 m*M* NaCl, pH 8.0, containing 500 m*M* imidazole.

2.3.2 Procedure

2.3.2.1 Expression and Purification of SLK-1-Containing Proteins

(a) Protein expression

1. Cotransform *E. coli* GH371 with plasmids pEVOL-PylRS_SL1 and a pBAD plasmid encoding the target gene with amber codons at the chosen position of SLK-1 incorporation under control of an araBAD promoter (e.g., pBAD-TRX_D14/R74TAG, pBAD-TRX_D14TAG, or pBAD-TRX_R74TAG) and select on LB agar plate supplemented with 34 μg/ml chloramphenicol and 50 μg/ml carbenicillin.
2. Inoculate a single clone in LB media supplemented with 34 μg/ml chloramphenicol and 50 μg/ml carbenicillin and grow overnight at 37 °C and 200 rpm shaking.
3. Dilute this culture 50-fold into fresh LB media supplemented with 34 μg/ml chloramphenicol and 50 μg/ml carbenicillin. Grow the culture at 37 °C and 200 rpm shaking and at an OD_{600} of 0.5–0.6, add 3 m*M* SLK-1 and induce with 0.2% (w/v) L-arabinose.
4. After 4 h growth under the same incubation conditions, harvest the culture by centrifugation (10 min, 3320 × *g*, room temperature, 4 °C). The pellet can be stored at −20 °C.

(b) Protein purification

1. Resuspend the pellet obtained from protein expression. For a 5 ml expression culture, use 500 μl B-Per lysis reagent containing 1 m*M* PMSF for resuspension. Incubate at 4 °C for 10 min with shaking.
2. Pellet the mixture by centrifugation (2 min, 20,817 × *g*, room temperature, 4 °C), recover the supernatant and add 10 μl 500 m*M*

imidazole and 50 µl Ni-NTA agarose slurry. Shake the suspension at 1000 rpm for 10 min at 4 °C and transfer to a paper filter spin column.

3. Centrifuge (106 × *g*, 10 s, room temperature) and wash resin 2 × with 500 µl, 4 × with PBS, and 2 × with 500 µl wash buffer by resuspension of the resin and centrifugation (106 × *g*, 10 s at room temperature).
4. Elute protein 3 × with 50 µl elution buffer by addition and centrifugation (1000 rpm, 10 s at room temperature).
5. Confirm the identity and analyze the purity of the obtained protein by SDS-PAGE and staining with Coomassie Brilliant Blue. Quantify using a BCA assay.
6. For EPR measurements, dialyze proteins 3 × against 10 m*M* Tris, pH 7.4, using a Slide-A-Lyzer dialysis column with 10 kDa MW cutoff.

2.4 EPR Measurements

2.4.1 EPR Spectrometers

For monitoring the integrity degree, a simple benchtop CW-EPR X-band spectrometer is sufficient. We usually use an X-band MiniScope spectrometer (MS200, magnettech GmbH) equipped with a variable temperature unit (Temperature Controller TC-H02, magnettech GmbH).

For increased sensitivity, it is recommended to perform the DEER experiments in Q-band. Cooling with liquid helium is useful because it optimizes sensitivity, but not a prerequisite for these measurements. Alternatively, liquid nitrogen can be used. We performed all EPR DEER experiments in Q-band at $T = 50$ K using an Elexsys E580 spectrometer (Bruker Biospin) with EN 5107D2 probehead, equipped with a helium gas flow system (CF935, Oxford Instruments).

2.4.2 Procedure

2.4.2.1 Monitoring Integrity Degrees by CW-EPR Measurements

1. Load samples into glass capillaries (Bluebrand, outer diameter 1 mm) with typical sample volumes of 20 µl.
2. Obtain CW-EPR spectra in liquid solution. Typical experimental parameters are a modulation amplitude of 800 mG and microwave attenuation of 15 dB of the microwave source ($P_0 = 100$ mW). The signal-to-noise ratio can be improved by accumulation of several spectra.

3. If required, the spectra can be analyzed using Matlab R2008b (The MatWorks, Inc.) and the toolbox EasySpin 2.6 (Stoll & Schweiger, 2006).
4. Determine signal intensities via the double integral of the first derivative EPR spectrum and can be compared to the obtained protein concentration.

2.4.2.2 DEER Experiments

1. The dead-time free four-pulse DEER sequence is shown in Fig. 5.
2. Estimate the required length of the measured dipolar evolution, which is approximately given by $t_{max} \approx \tau_2$ (where t_{max} is the maximum dipolar evolution time and τ_2 is the separation time between the primary echo and the second π pulse of the observer sequence). The required t_{max} depends on the expected value of the distance to be measured. With $t_{max} = 2$ μs, the shape of the distance distribution is reliable up to a distance of 3 nm (reliable distribution limit). The mean distance and the width of its distribution are reliable up to a distance of 4 nm (reliable width limit), whereas the mean distance, but not the distribution width, is reliable between 4 and 5 nm (reliable mean distance limit). Beyond 5 nm no reliable mean value can be determined. All these limits scale with the cubic root of t_{max} (Jeschke, Chechik, et al., 2006; Stoll & Schweiger, 2006).
3. Cool the cryostat down to a working temperature of 50 K. Readjust the resonant microwave frequency to the center of the resonator if necessary. This is the pump frequency.
4. Apply the Hahn-echo sequence $\pi/2$–τ–π–τ–echo ($\pi/2$ and π pulses are typically 16 and 32 ns long, respectively, and $\tau = 300$ ns). Adjust shot repetition time, video amplifier bandwidth, microwave attenuation, and magnetic field, phase to maximize the echo.

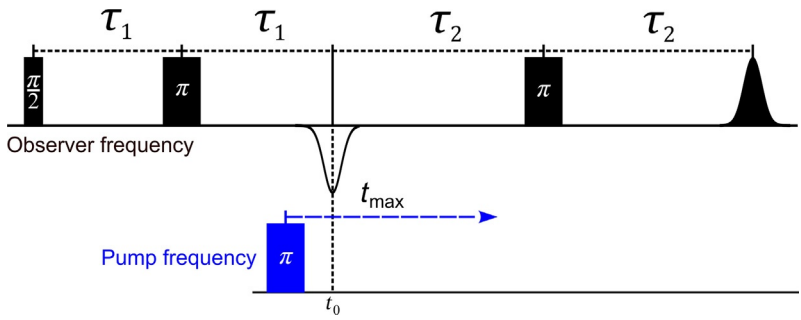

Figure 5 Scheme of dead-time free, four-pulse DEER sequence.

5. To adjust the pump pulse at this microwave frequency (pump frequency), use the inversion recovery pulse sequence π–τ_1–$\pi/2$–τ_2–π–τ_2–echo. The first π pulse is applied via the ELDOR channel, its frequency is set to the pump frequency. This pulse is placed 400 ns before the Hahn-echo sequence. Optimize the ELDOR channel π-pulse length to have maximum negative echo amplitude corresponding to inversion.
6. Set the operating frequency 50 MHz lower than the pump frequency. This value is defined as the observer frequency. Apply the Hahn-echo sequence $\pi/2$–τ–π–τ–echo ($\tau = 300$ ns) for $+\langle x\rangle$ and $-\langle x\rangle$ channels. Maximize the echo intensity by varying the pulse length at zero attenuation. Adjust the phases so as to observe a phase shift of 180° between the two-pulse channels.
7. Apply the $\pi/2$–τ_1–π–τ_1–echo–τ_2–π–τ_2–refocused echo sequence at the observer frequency ($\tau_1 = 300$ ns, τ_2 initial value = 1 μs). Set the SpecJet scale factor to one. Adjust τ_2 by inspecting the refocused echo. Set τ_2 to the longest value at which the refocused echo can still be clearly recognized. Typical values are between 1 and 3.5 μs.
8. Apply the DEER sequence (Fig. 5). The pump inversion pulse (at the pump frequency on resonance with the microwave cavity) with a length determined in step 5 starts with a delay time $<2\tau_1$, but large enough not to overlap with the first observer π pulse. The pump pulse is swept within the experiment in 8 ns steps resulting in the DEER trace.
9. Set the phase cycle for the observer sequence to be: $\pi/2(+\langle x\rangle)$–$\pi(\langle y\rangle)$–$\pi(\langle y\rangle)$ and $\pi/2(-\langle x\rangle)$–$\pi(\langle y\rangle)$–$\pi(\langle y\rangle)$.
10. For deuterated samples, apply nuclear modulation suppression by averaging DEER traces for 10 different τ_1 values incremented by 8 ns.
11. Set the integration window symmetrically over the refocused echo.
12. Set the number of averages for the SpecJet to 1. Adjust the gain so that the signal intensity does not exceed the SpecJet window.
13. Increase the number of scans and shots per point to repeat the experiment as often as required to obtain an acceptable signal-to-noise ratio. Depending on spectrometer stability, one should not exceed accumulation times of 24 h. We usually use 18 h.

2.4.3 Analysis of DEER Data

1. Install DeerAnalysis 2013.2 in your Matlab environment following the instructions in the user manual. Perform the data analysis according to the DeerAnalysis manual (http://www.epr.ethz.ch/software).

2. Use an experimental background function derived from the individually measured DEER traces of the protein with a single SLK-1 incorporated.
3. Extract the distance distribution for the doubly labeled protein with the model-free Tikhonov regularization method (Chiang, Borbat, & Freed, 2005; Stoll & Schweiger, 2006). The modulation depth of the DEER curve might be significantly depressed by chemical reduction of the spin label.
4. In order to systematically analyze the influence of the different steps in the signal treatment process (baseline correction, signal-to-noise ratio, choice of regularization parameter, etc.) on the results of Tikhonov regularization, conduct systematic variation of parameters and monitoring changes in the resulting distance distribution using the DeerAnalysis software. Since the uncertainties in the parameters discussed above may be correlated, a statistical analysis of the distance distribution obtained by variations in a multidimensional parameter space is required. A thorough analysis monitoring the uncertainties in different steps of the data postprocessing (starting time of the background fitting, period of background fitting, background density, white noise) allows for validation of the presented distance distributions.

ACKNOWLEDGMENTS

M.J.S. acknowledges a Hoechst Fellowship of the Aventis Foundation. This work was supported the DFG within SPP1601.

REFERENCES

Altenbach, C., Marti, T., Khorana, H. G., & Hubbell, W. L. (1990). Transmembrane protein structure: Spin labeling of bacteriorhodopsin mutants. *Science*, *248*(4959), 1088.

Azarkh, M., Okle, O., Singh, V., Seemann, I. T., Hartig, J. S., Dietrich, D. R., et al. (2011). Long-range distance determination in a DNA model system inside Xenopus laevis oocytes by in-cell spin-label EPR. *ChemBioChem*, *12*(13), 1992.

Azarkh, M., Singh, V., Okle, O., Dietrich, D. R., Hartig, J. S., & Drescher, M. (2012). Intracellular conformations of human telomeric quadruplexes studied by electron paramagnetic resonance spectroscopy. *ChemPhysChem*, *13*(6), 1444.

Azarkh, M., Singh, V., Okle, O., Seemann, I. T., Dietrich, D. R., Hartig, J. S., et al. (2013). Site-directed spin-labeling of nucleotides and the use of in-cell EPR to determine long-range distances in a biologically relevant environment. *Nature Protocols*, *8*(1), 131.

Baldauf, C., Schulze, K., Lueders, P., Bordignon, E., & Tampe, R. (2013). In-situ spin labeling of his-tagged proteins: Distance measurements under in-cell conditions. *Chemistry*, *19*(41), 13714–13719.

Belkin, S., Mehlhorn, R. J., Hideg, K., Hankovsky, O., & Packer, L. (1987). Reduction and destruction rates of nitroxide spin probes. *Archives of Biochemistry and Biophysics*, *256*(1), 232.

Blight, S. K., Larue, R. C., Mahapatra, A., Longstaff, D. G., Chang, E., Zhao, G., et al. (2004). Direct charging of tRNA(CUA) with pyrrolysine in vitro and in vivo. *Nature*, *431*(7006), 333.

Cellitti, S. E., Jones, D. H., Lagpacan, L., Hao, X., Zhang, Q., Hu, H., et al. (2008). In vivo incorporation of unnatural amino acids to probe structure, dynamics, and ligand binding in a large protein by nuclear magnetic resonance spectroscopy. *Journal of the American Chemical Society*, *130*(29), 9268–9281.

Chatterjee, A., Sun, S. B., Furman, J. L., Xiao, H., & Schultz, P. G. (2013). A versatile platform for single- and multiple-unnatural amino acid mutagenesis in Escherichia coli. *Biochemistry*, *52*, 1828–1837.

Chen, P. R., Groff, D., Guo, J. T., Ou, W. J., Cellitti, S., Geierstanger, B. H., et al. (2009). A facile system for encoding unnatural amino acids in mammalian cells. *Angewandte Chemie (International Ed. in English)*, *48*(22), 4052–4055.

Chiang, Y. W., Borbat, P. P., & Freed, J. H. (2005). The determination of pair distance distributions by pulsed ESR using Tikhonov regularization. *Journal of Magnetic Resonance*, *172*(2), 279–295.

Cornish, V. W., Benson, D. R., Altenbach, C. A., Hideg, K., Hubbell, W. L., & Schultz, P. G. (1994). Site-specific incorporation of biophysical probes into proteins. *Proceedings of the National Academy of Sciences of the United States of America*, *91*(8), 2910.

Couet, W. R., Brasch, R. C., Sosnovsky, G., & Tozer, T. N. (1985). Factors affecting nitroxide reduction in ascorbate solution and tissue homogenates. *Magnetic Resonance Imaging*, *3*(1), 83.

Fekner, T., Li, X., Lee, M. M., & Chan, M. K. (2009). A pyrrolysine analogue for protein click chemistry. *Angewandte Chemie (International Ed. in English)*, *48*(9), 1633.

Fleissner, M. R., Brustad, E. M., Kalai, T., Altenbach, C., Cascio, D., Peters, F. B., et al. (2009). Site-directed spin labeling of a genetically encoded unnatural amino acid. *Proceedings of the National Academy of Sciences of the United States of America*, *106*(51), 21637.

Gautier, A., Nguyen, D. P., Lusic, H., An, W. A., Deiters, A., & Chin, J. W. (2010). Genetically encoded photocontrol of protein localization in mammalian cells. *Journal of the American Chemical Society*, *132*(12), 4086.

Guo, J., Melancon, C. E., 3rd, Lee, H. S., Groff, D., & Schultz, P. G. (2009). Evolution of amber suppressor tRNAs for efficient bacterial production of proteins containing nonnatural amino acids. *Angewandte Chemie (International Ed. in English)*, *48*(48), 9148–9151.

Hoppmann, C., Lacey, V. K., Louie, G. V., Wei, J., Noel, J. P., & Wang, L. (2014). Genetically encoding photoswitchable click amino acids in Escherichia coli and mammalian cells. *Angewandte Chemie (International Ed. in English)*, *53*(15), 3932–3936.

Huang, Y., Russell, W. K., Wan, W., Pai, P. J., Russell, D. H., & Liu, W. (2010). A convenient method for genetic incorporation of multiple noncanonical amino acids into one protein in Escherichia coli. *Molecular BioSystems*, *6*(4), 683–686.

Hubbell, W. L., Cafiso, D. S., & Altenbach, C. (2000). Identifying conformational changes with site-directed spin labeling. *Nature Structural Biology*, *7*(9), 735.

Igarashi, R., Sakai, T., Hara, H., Tenno, T., Tanaka, T., Tochio, H., et al. (2010). Distance determination in proteins inside Xenopus laevis oocytes by double electron–electron resonance experiments. *Journal of the American Chemical Society*, *132*(24), 8228.

Jeschke, G. (2002). Distance measurements in the nanometer range by pulse EPR. *ChemPhysChem*, *3*(11), 927–932.

Jeschke, G. (2012). DEER distance measurements on proteins. *Annual Review of Physical Chemistry*, *63*, 419.

Jeschke, G., Abbott, R. J. M., Lea, S. M., Timmel, C. R., & Banham, J. E. (2006). The characterization of weak protein-protein interactions: Evidence from DEER for the trimerization of a von Willebrand factor A domain in solution. *Angewandte Chemie (International Ed. in English)*, *45*(7), 1058–1061.

Jeschke, G., Bender, A., Paulsen, H., Zimmermann, H., & Godt, A. (2004). Sensitivity enhancement in pulse EPR distance measurements. *Journal of Magnetic Resonance*, *169*(1), 1–12.

Jeschke, G., Chechik, V., Ionita, P., Godt, A., Zimmermann, H., Banham, J., et al. (2006). DeerAnalysis2006—A comprehensive software package for analyzing pulsed ELDOR data. *Applied Magnetic Resonance*, *30*(3–4), 473–498.

Johnson, D. B. F., Wang, C., Xu, J. F., Schultz, M. D., Schmitz, R. J., Ecker, J. R., et al. (2012). Release factor one is nonessential in Escherichia coli. *ACS Chemical Biology*, *7*(8), 1337.

Johnson, D. B., Xu, J., Shen, Z., Takimoto, J. K., Schultz, M. D., Schmitz, R. J., et al. (2011). RF1 knockout allows ribosomal incorporation of unnatural amino acids at multiple sites. *Nature Chemical Biology*, *7*(11), 779.

Kalai, T., Fleissner, M. R., Jeko, J., Hubbell, W. L., & Hideg, K. (2011). Synthesis of new spin labels for Cu-free click conjugation. *Tetrahedron Letters*, *52*(21), 2747–2749.

Katti, S. K., LeMaster, D. M., & Eklund, H. (1990). Crystal structure of thioredoxin from Escherichia coli at 1.68 Å resolution. *Journal of Molecular Biology*, *212*(1), 167–184.

Klare, J. P., & Steinhoff, H. J. (2009). Spin labeling EPR. *Photosynthesis Research*, *102*(2–3), 377.

Krstic, I., Hansel, R., Romainczyk, O., Engels, J. W., Dotsch, V., & Prisner, T. F. (2011). Long-range distance measurements on nucleic acids in cells by pulsed EPR spectroscopy. *Angewandte Chemie (International Ed. in English)*, *50*(22), 5070.

Lajoie, M. J., Rovner, A. J., Goodman, D. B., Aerni, H. R., Haimovich, A. D., Kuznetsov, G., et al. (2013). Genomically recoded organisms expand biological functions. *Science*, *342*(6156), 357–360.

Li, F., Zhang, H., Sun, Y., Pan, Y., Zhou, J., & Wang, J. (2013). Expanding the genetic code for photoclick chemistry in E. coli, mammalian cells, and A. thaliana. *Angewandte Chemie (International Ed. in English)*, *52*(37), 9700–9704.

Liu, C. C., & Schultz, P. G. (2010). Adding new chemistries to the genetic code. *Annual Review of Biochemistry*, *79*, 413.

Luo, J., Uprety, R., Naro, Y., Chou, C., Nguyen, D. P., Chin, J. W., et al. (2014). Genetically encoded optochemical probes for simultaneous fluorescence reporting and light activation of protein function with two-photon excitation. *Journal of the American Chemical Society*, *136*(44), 15551–15558.

Martorana, A., Bellapadrona, G., Feintuch, A., Di Gregorio, E., Aime, S., & Goldfarb, D. (2014). Probing protein conformation in cells by EPR distance measurements using Gd3+ spin labeling. *Journal of the American Chemical Society*, *136*(38), 13458–13465.

Mukai, T., Hayashi, A., Iraha, F., Sato, A., Ohtake, K., Yokoyama, S., et al. (2010). Codon reassignment in the Escherichia coli genetic code. *Nucleic Acids Research*, *38*(22), 8188–8195.

Pace, N. J., & Weerapana, E. (2013). Diverse functional roles of reactive cysteines. *ACS Chemical Biology*, *8*(2), 283–296.

Plass, T., Milles, S., Koehler, C., Szymanski, J., Mueller, R., Wiessler, M., et al. (2012). Amino acids for diels-alder reactions in living cells. *Angewandte Chemie (International Ed. in English)*, *51*(17), 4166–4170.

Polycarpo, C. R., Herring, S., Berube, A., Wood, J. L., Soll, D., & Ambrogelly, A. (2006). Pyrrolysine analogues as substrates for pyrrolysyl-tRNA synthetase. *FEBS Letters*, *580*(28–29), 6695.

Polyhach, Y., Bordignon, E., & Jeschke, G. (2011). Rotamer libraries of spin labelled cysteines for protein studies. *Physical Chemistry Chemical Physics*, *13*(6), 2356–2366.

Pott, M., Schmidt, M. J., & Summerer, D. (2014). Evolved sequence contexts for highly efficient amber suppression with noncanonical amino acids. *ACS Chemical Biology*, *9*(12), 2815–2822.

Qi, M., Groß, A., Jeschke, G., Godt, A., & Drescher, M. (2014). Gd(III)-PyMTA label is suitable for in-cell EPR. *Journal of the American Chemical Society*, *136*(43), 15366–15378.

Ryden, S. M., & Isaksson, L. A. (1984). A temperature-sensitive mutant of Escherichia coli that shows enhanced misreading of UAG/A and increased efficiency for some transfer-RNA nonsense suppressors. *Molecular & General Genetics*, *193*(1), 38–45.

Ryu, Y., & Schultz, P. G. (2006). Efficient incorporation of unnatural amino acids into proteins in Escherichia coli. *Nature Methods*, *3*(4), 263–265.

Schmidt, M. J., Borbas, J., Drescher, M., & Summerer, D. (2014). A genetically encoded spin label for electron paramagnetic resonance distance measurements. *Journal of the American Chemical Society*, *136*(4), 1238–1241.

Schmidt, M. J., & Summerer, D. (2013). Red-light-controlled protein-RNA crosslinking with a genetically encoded furan. *Angewandte Chemie (International Ed. in English)*, *52*(17), 4690.

Shafer, A. M., Kalai, T., Liu, S. Q. B., Hideg, K., & Voss, J. C. (2004). Site-specific insertion of spin-labeled L-amino acids in Xenopus oocytes. *Biochemistry*, *43*(26), 8470.

Stoll, S., & Schweiger, A. (2006). EasySpin, a comprehensive software package for spectral simulation and analysis in EPR. *Journal of Magnetic Resonance*, *178*(1), 42–55.

Wan, W., Huang, Y., Wang, Z. Y., Russell, W. K., Pai, P. J., Russell, D. H., et al. (2010). A facile system for genetic incorporation of two different noncanonical amino acids into one protein in Escherichia coli. *Angewandte Chemie (International Ed. in English)*, *49*(18), 3211–3214.

Wan, W., Tharp, J. M., & Liu, W. R. (2014). Pyrrolysyl-tRNA synthetase: An ordinary enzyme but an outstanding genetic code expansion tool. *Biochimica et Biophysica Acta*, *1844*(6), 1059–1070.

Wang, K. H., Neumann, H., Peak-Chew, S. Y., & Chin, J. W. (2007). Evolved orthogonal ribosomes enhance the efficiency of synthetic genetic code expansion. *Nature Biotechnology*, *25*(7), 770–777.

Wu, I. L., Patterson, M. A., Carpenter Desai, H. E., Mehl, R. A., Giorgi, G., & Conticello, V. P. (2013). Multiple site-selective insertions of noncanonical amino acids into sequence-repetitive polypeptides. *ChemBioChem*, *14*(8), 968–978.

Yanagisawa, T., Ishii, R., Fukunaga, R., Kobayashi, T., Sakamoto, K., & Yokoyama, S. (2008). Multistep engineering of pyrrolysyl-tRNA synthetase to genetically encode N(epsilon)-(o-azidobenzyloxycarbonyl) lysine for site-specific protein modification. *Chemistry & Biology*, *15*(11), 1187.

Young, T. S., Ahmad, I., Yin, J. A., & Schultz, P. G. (2010). An enhanced system for unnatural amino acid mutagenesis in E. coli. *Journal of Molecular Biology*, *395*(2), 361–374.

Zhang, S., Ryden-Aulin, M., Kirsebom, L. A., & Isaksson, L. A. (1994). Genetic implication for an interaction between release factor one and ribosomal protein L7/L12 in vivo. *Journal of Molecular Biology*, *242*(5), 614–618.